Impact of Cascading and Common-Cause Outages on Resilience-Constrained Optimal Economic Operation of Power Systems

Yifei Wang, *Member, IEEE*, Liping Huang, *Student Member, IEEE*, Mohammad Shahidehpour, *Fellow, IEEE*, Loi Lei Lai, *Fellow, IEEE*, and Ya Zhou, *Member, IEEE*

***Abstract*—Common-cause and cascading outages in extreme power system conditions may challenge traditional N-k transmission security strategies. This paper proposes a resilience index (RI) to evaluate the power system adaptability to extreme conditions and establishes the resilience-constrained economic dispatch (RCED) model and solution methodology in power system operations. A three-stage outage sampling method is presented to assess the proposed RI in severe weather conditions culminating in common-cause and cascading outages. In the proposed RCED model, customized contingency constraints are introduced to represent common-cause and cascading outages in extreme events and two penalty terms are considered that can adjust power transmission flows for lowering outage risks in a power grid. An optimization method is presented to solve the RCED model efficiently with an absolute value function introduced in both objective function and constraints. A sufficient and necessary condition is proposed to ensure the optimality of the linearized solution is the same as that of the original problem. Case studies show the effectiveness of the proposed model and methodology.**

***Index Terms*—Power system resilience, cascading outages, common-cause outages, resilience-constrained economic dispatch, absolute value function.**

NOMENCLATURE

Variables and Functions

$C_i(\cdot)$	Fuel consumption function of unit i
LC_j	Curtailment at load j
i	Index for generator unit
j	Index for bus load
l, p, q	Index for transmission line
P_i	Generation of unit i
PL_l	Real power flow of line l
PL_l^{pc}	Line l flow for an outage on line p
$PL_l^{p-q,c}$	Line l flow for common-cause outages on lines p and q
p_k^{cf}	Weather-dependent outage probabilities of conductor k
p_k^{tf}	Weather-dependent outage probabilities of tower k
p_l^{wf}	Weather-dependent outage probabilities of transmission line l
$p_{p,q}^{cco}$	Probability of common-cause outage of line p and q
p_l^{hf}	Hidden outage probability of line l
r_l	Absolute loading rate of line l
s_l, t_l	Auxiliary variables to linearize (15o)
u_l, v_l	Auxiliary variables to linearize (9a)
σ_l	Auxiliary binary variables to linearize (9c).

Constants and Sets

α	Coefficient of generation cost
β	Coefficient of the first penalty term
γ	Coefficient of the second penalty term
η	Coefficient of the load curtailment
PD_j	Real transmission load j
KD	Bus-load incidence matrix
KL	Bus-line incidence matrix
KP	Bus-generator incidence matrix
NL	Number of total transmission lines
NG	Number of generation units
ND	Number of transmission loads
NC_l	Number of conductors on line l
NT_l	Number of towers connected to line l
$P_{\min,i}$	Lower power generation limit of unit i
$P_{\max,i}$	Upper power generation limit of unit i
$PL_{\max,l}$	Capacity limit of line l
S_{AL}	Set of extreme weather affected lines.

Manuscript received September 7, 2018; revised February 11, 2019 and May 28, 2019; accepted May 31, 2019. Date of publication July 1, 2019; date of current version December 23, 2019. This work was supported in part by the Department of Finance and Education of Guangdong Province 2016[202]: Key Discipline Construction Program, China and Education Department of Guangdong Province: New and Integrated Energy System Theory and Technology Research Group under Project 2016KCXTD022, in part by the Natural Science Foundation of China under Grant 71704029, and in part by the State Grid Henan Electric Power Company under Grant 5217901800RQ. Paper no. TSG-01311-2018. *(Corresponding authors: Mohammad Shahidehpour; Loi Lei Lai; Ya Zhou.)*

Y. Wang is with Southeast University, Nanjing 210096, China.

L. Huang, L. L. Lai, and Y. Zhou are with the Department of Electrical Engineering, Guangdong University of Technology, Guangzhou 510006, China (e-mail: l.l.lai@gdut.edu.cn; yazhou@gdut.edu.cn).

M. Shahidehpour is with the Electrical and Computer Engineering Department, Illinois Institute of Technology, Chicago, IL 60616 USA, and also with ECE Department, King Abdulaziz University, Jeddah 21589, Saudi Arabia (e-mail: ms@iit.edu).

Color versions of one or more of the figures in this paper are available online at http://ieeexplore.ieee.org.

Digital Object Identifier 10.1109/TSG.2019.2926241

I. INTRODUCTION

COMMON-CAUSE outages refer to simultaneous outages of multiple components due to a common event [1]. For

example, outages of two or more circuits on the same transmission tower can occur due to a single incident and the outage of multiple lines on the same substation due to a lightning invasion can wave overvoltage accidents. Also, a major physical disturbance such as tornado can result in outages of two or more transmission circuits on the same right-of-way. Such outages can be classified as common-cause outages since a single cause results in an outage of two or more elements [2], [3]. Traditionally, common-cause outages are regarded as small probability events and mostly ignored. However, the possibility of common-cause outages under extreme events are higher than that in normal conditions. As a result, the possibility of system blackout could dramatically be increased upon common-cause outages. In this paper, we only consider common-cause outages of two transmission lines which are in a common right-of-way or connected to the same bus which are in extreme events.

An increasing number of cascading outages in extreme conditions indicate that power system vulnerabilities are continuously exposed to serious weather conditions which could culminate in extensive power blackouts. Resilience would evaluate the performance of an ecosystem affected by external changes and continually confronted by unexpected events. Similarly, power system resilience describes the capability of power systems to change itself to withstand major events with high-impact and low-probability [4]–[6].

Cascading outages with inherently complex nature could have a compounded effect on power system operations. Some references linked power system operating conditions to cascading outages. Reference [7] demonstrated that self-organized criticality is an essential characteristic of large blackouts. Reference [8] illustrated that power system loading that is close to the system operating limits is the key outage attribute that could lead to cascading outages. According to the system structure and operating states, [9] proposed an entropy-based metric to evaluate the power grid robustness with respect to cascading outages. Reference [10] showed the correlations between self-organized criticality and the heterogeneity of power flow distribution by introducing the power flow entropy index. Accordingly, the larger the power flow entropy, the more routinely a power system state can lead to self-organized criticality and eventually lead to cascading outages.

Fig. 1 shows a typical power system resilience curve which is divided into three development stages, i.e., adaptation, absorption and restoration, with specific resilience indices [11]–[13]. For example, the *BC* slope denotes how fast the system deteriorates, *CD* segment denotes the system robustness, *DF* segment denotes how promptly the network recovers, and *BCDEF* area denotes the system loss. According to the definition of power system resilience, the adaptation in Fig. 1 describes the power system capability to adapt to prevailing conditions in response to unexpected events. However, the adaptation stage lacks indices that describe the adaptive capacity of power systems in extreme events which may lead to cascading outages.

To improve the power system resilience, a comprehensive operation strategy is needed where the power flow distribution and customized contingencies in extreme events are addressed

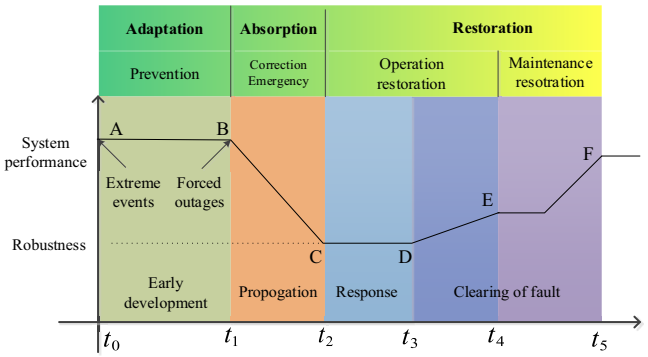

Fig. 1. Typical resilience curve.

simultaneously. In this paper, we introduce a new resilience index (RI) to describe adaptation performance and establish a preventive resilience-constrained economic dispatch (RCED) strategy to improve power system adaptability. The proposed approach fills the gap in which penalty terms and customized contingency constraints are established by considering extreme events to improve the uniformity of power flow distribution, reduce the impacts of common-cause and cascading outages, and boost the system adaptability to extreme events.

Some previous studies proposed preventive strategies for enhancing the power system resilience. In [14], a sequential proactive operation strategy was proposed where the system state transition follows a Markov process. Reference [15] considered cascading outages and N-k contingencies to establish a risk-based operation strategy. In [16], an N-k contingency screening method for economic dispatch was proposed with multi-objective optimization where the maximized level of system load shedding and the minimized number of contingencies were considered. In [17], the outage set for economic dispatch were constructed based on risk assessments in a bi-level framework.

Reference [18] studied the proactive microgrid dispatch strategy to enhance resilience in which the islanded operation time is modeled as uncertainty set. To further enhance power system resilience, [19] studied the power system economic dispatch integrated with microgrids in extreme conditions. Reference [20] proposed the optimal resilience operation in terms of line hardening. Different hardening methods were determined to reduce line outage probabilities and load shedding costs. Reference [21] studied the resilience enhancement strategy considering the line hardening and the formation of multiple islanded provisional microgrids. Reference [22] proposed an N-k contingency screening method considering the hidden outages. Reference [23] proposed an approach to construct contingency constraints using line outage distribution factors (LODFs) to reduce the computational burdens. Reference [24] established a robust model for extreme events to achieve the optimal hardening strategy in integrated electricity and nature gas transportation systems.

The previous references studied the power system resilience and security considering N-k contingencies. Such resilience operation strategies could improve the system performance towards specific contingencies. These studies have had an implicit assumption that improving the power system

reliability, such as implementing the N-k contingencies, could lead to more resilient power system operations at certain circumstances. This view may be true when a power system is subject to typical outages. However, when a power system is subject to extreme conditions, such as severe weather with common-cause outages and cascading outages, the traditional N-*k* reliability security strategies may not be effective.

In extreme situations, power system operation characteristics and forced outage modes could change [25]. Forced outages occur randomly with certain effects on reliability, but presumed outages could be much more profound if they demonstrate cascading effects and outage correlations in extreme circumstances. Moreover, contingencies representing typical power system outages would usually be more complicated in extreme events due to the extent of common-cause outages and cascading outages. Thus, if reliability-based operation strategies are instituted without considering the unique features of extreme events, the severe impacts of cascading outages, could more readily culminate the power system in blackouts (e.g., North America on August 14, 2003, Europe on November 12, 2006, Brazil on November 10, 2009, and India on July 30, 2012). To enhance the system resilience, we consider common-cause and cascading outages along with single outages in the resilience-based operation strategy.

Our earlier work [26] presented a resilience-constrained unit commitment model where the power flow entropy was considered to improve the power system resilience. The main difference between the model in [26] and that in this paper lies in the following points. First, new penalty terms are proposed in this paper which are much smaller and less cumbersome than those in [26], which lead to better computation performances. Second, the convexification method of penalty terms are different. An approximation method was considered which reduced the solution optimality in [26]. In this paper, we establish a transformed problem to solve the original problem and prove that the two problems are equivalent when the proposed necessary and sufficient condition is satisfied. In this paper, a new outage set containing three types of events is established for enhancing RCED. Furthermore, a new RI is proposed to reflect the adaptability of power systems to extreme conditions.

The main contributions of this work are summarized below.

- Considering common-cause and cascading outages, a new RI is proposed to quantify the power system adaptability to extreme events. RI is utilized at the adaption stage.
- An RCED model for blackout prevention and resilience enhancement is presented in which the system security subjected to common-cause outages and cascading outages is addressed simultaneously. Two penalty terms are introduced to improve the system resilience under hidden cascading outages. The common-cause outages and cascading outages types of contingencies are evaluated to improve the power system performance under reliability types of outages.
- A convexification method is proposed to linearize the RCED model without the loss of optimality. Although the linearized problem is not equivalent to the original one, a sufficient and necessary condition is introduced to ensure that the optimal value of linearized problem is the same as that of the original problem.

This paper is organized as follows, Section II describes the proposed cascading-based RI for resilience evaluation. Section III introduces the proposed resilience constrained economic dispatch and its convexification solution. Section IV presents the case studies, and the work is concluded in Section V.

II. Resilience Evaluation for Cascading Outages

The proposed outage set will not include all common-cause contingencies. The established outage set contains three stages. First, the N-1 contingency for weather-affected lines are added to reduce the impact of weather-induced initial outages. Second, common-cause outages for weather-affected lines are added. Third, heavily loaded lines upon the weather-induced initial outages are identified. To avoid the risk of hidden and cascading outages, each heavily loaded line and corresponding initial lines on outage are identified as contingency events. For each outage, the corresponding constraints are established and added to the RCED model using line outage distribution factor (LODF). At present, it is not possible to guarantee that load demands are always satisfied in contingencies. When the power system is subject to extreme weather events, the operator may shed some load or send demand response signals to improve the power flow distribution, reduce cascading outage risk and enhance system resilience.

A. Random Outages in Extreme Conditions

The proposed process for considering random outages in power systems includes three stages. The first stage considers extreme events, such as severe weather conditions, to determine initial line outages. The second stage considers common-cause outages in lines that are adjacent to initial outages. The third stage considers cascading outages in which a simulation model is introduced to determine whether the remaining lines are subject to cascading outages. The details of each state are as follows.

1) Weather-Induced Initial Line Outages: Without the loss of generality, we apply the generic wind-related fragility curves for transmission lines and towers [11]. For a real power system, the fragility function of each component in different weather conditions can be derived empirically from statistical analysis based on observed failures. The wind speed is obtained from meteorological department or derived from prevailing wind model simulations. Assume the failure probability of a single conductor and tower are p^{cf} and p^{tf}, respectively. Since individual failure of a conductor and transmission tower both will lead to outage of a transmission line, the outage probability of a transmission line structure is

$$p_l^{wf} = 1 - \prod_{k=1}^{Nc_l}\left(1 - p_k^{cf}\right) \cdot \prod_{k=1}^{Nt_l}\left(1 - p_k^{tf}\right). \tag{1}$$

2) Common-Cause Outages: In practice, common-cause outages occur when one event causes multiple outages which are not statistically independent. In this paper, we only consider the common-cause outages of adjacent components in

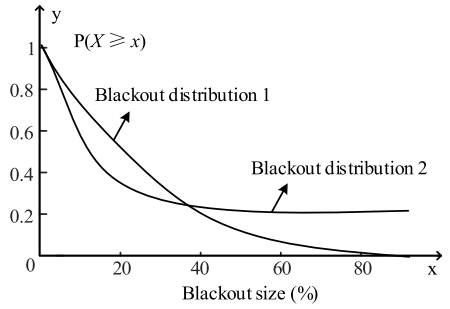

Fig. 2. Two blackout distributions.

weather affected areas. The two lines could be either on a common right-of-way or connected with the same bus. The common-cause outages of transmission lines p and q are stated as [27].

$$p_{p,q}^{cco} = \frac{\mu_p \mu_q \lambda_{p,q}^c}{(\mu_p + \lambda_p)(\mu_q + \lambda_q)\mu_{p,q}^c + \mu_p \mu_q \lambda_{p,q}^c} \tag{2}$$

where λ_p and λ_q are the failure rate (failures/year) of transmission lines p and q, respectively; μ_p and μ_q are the repair rate (repairs/year) of transmission lines p and q, respectively; $\lambda_{p,q}^c$ and $\mu_{p,q}^c$ are the common-cause failure and repair rates of the transmission lines p and q, respectively.

3) Hidden Outages: A hidden outage remains undetected in normal operating conditions but exposed after the occurrence of a power system disturbance, which may cause relays to trip erroneously [28]. According to [29], [30], the components connected to tripped lines would also be exposed to incorrect tripping. The hidden outage probability, which has an approximate linear relationship with the line loading when the corresponding flow exceeds its limit [28], is stated as

$$p_l^{hf} = \begin{cases} p_0, & 0 \le r_l \le 1 \\ k_0 \cdot r_l + b, & 1 \le r_l \le r_l^t \\ 1, & r_l \ge r_l^t \end{cases} \tag{3}$$

where p_0 is the initial hidden outage probability which depends on line parameters, k_0 and b are the coefficients of the linear function, and r_l^t is the thermal limit of line l.

B. Proposed Resilience Evaluation Indices

Fig. 2 shows two different complementary cumulative distribution function (CCDF) of blackout size distribution of a system in different operating strategies, where x could be any blackout measure, such as load curtailment percentage, tripped lines percentage, y is the probability of $X \ge x$. Initially, curve 1 drops more sharply as blackout gets larger, which indicates that curve 1 has higher proportion of small accidents but fewer major accidents. On the contrast, curve 2 has a relatively flat tail which means that curve 2 has a higher proportion of large accidents but fewer small accidents. Therefore, from the perspective of preventing large blackout in extreme conditions, the first operational strategy is more resilient.

However, reliability indices, such as the expected load curtailment, may be similar for the two strategies. Therefore, traditional reliability evaluation indices underestimate the risk of large blackout which are not suitable for the system resilience evaluation. Resilience considers the system performance in extreme events, which cannot evaluated effectively by conventional reliability indices. To fill the gap, we propose a new RI as

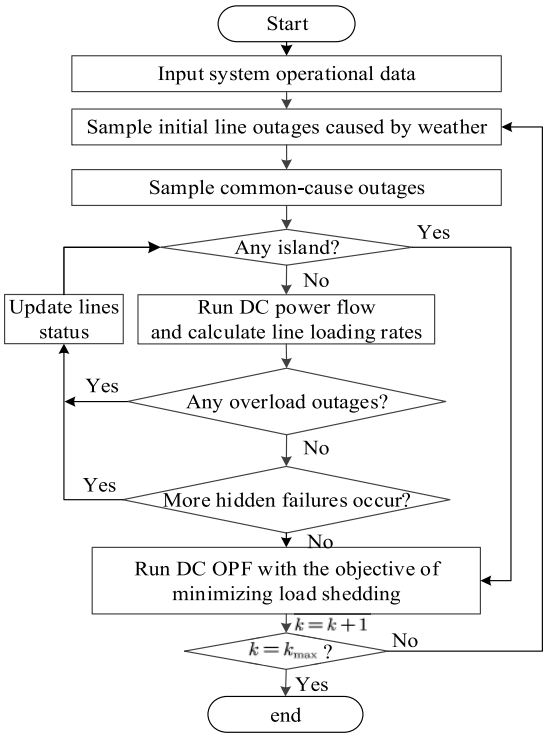

Fig. 3. Proposed resilience evaluation method.

$$RI = \sum_{k=1}^{NX} x_k \cdot P(X \ge x_k) \tag{4}$$

where NX is the number of points to evaluate (4). In this paper, $NX = 100$. RI is evaluated by changing x_k from 0 to 100 (percent), which ensures that large blackouts with a larger outage impact are represented by larger RI (though the two expected load curtailment are similar). The incremental RI considering two different strategies is stated as

$$\Delta\ RI = RI_2 - RI_1 = \left(\sum_{k=1}^{NI} x_k \cdot (P_2(X \ge x_k) - P_1(X \ge x_k)) \right) \tag{5}$$

In this paper, the blackout size x in (4) and (5) is defined as load curtailment/system load which is dimensionless. Thus, RI is dimensionless. To calculate RI, the input data include power system parameters, forecasted weather in affected areas, dispatch conditions, and outage characteristics. The output data includes RI, sampled scenarios, and probability distribution of load curtailment.

To calculate x, we apply the Monte Carlo technique to the proposed resilience evaluation method. The overall flowchart for the proposed simulation process is shown in Fig. 3. For each Monte Carlo simulation:

1) Sample weather-related initial line outages according to (1). The initial tripped transmission lines are simulated by comparing p_l^{wf} with a uniformly distributed random number $\rho_1 \sim U(0, 1)$. Trip line l if $p_l^{wf} > \rho_1$.

2) Sample common-cause outages adjacent to initial line outages according to (2). Compare $p_{p,q}^{cco}$ with $\rho_2(\rho_2 \sim U(0,1))$, and trip lines p and q if $p_{p,q}^{cco} > \rho_2$.
3) Check network connectivity by calculating the blackout size in each island if the network is partitioned; then end the process. Otherwise, go to Step 4.
4) Calculate power flow and check thermal limit violations. Trip the lines with load rates exceeding r_l^t.
5) Sample hidden outages. Identify lines connected to tripped lines and calculate hidden outage probability according to (3). Trip individual lines if $p_l^{htf} > \rho_3(\rho_3 \sim U(0,1))$. Go to Step 3.

III. The Proposed RCED Model

A. Penalty Terms Based on Power Flow Entropy

The power flow entropy provides a measure of power flow distribution uniformity. Reference [10] showed that the power flow entropy has a close relation with the blackout size in cascading outages. When the entropy is high, transmission lines which carry heavy loads can fail and trigger cascading outages more easily.

However, it is difficult to optimize the power flow entropy directly in a mathematical programming model. Therefore, to reduce the power flow entropy and homogenize the power flow distribution, we consider two penalty terms as

$$pn_1 = \sum_{l \in S_{AL}} \left| \frac{PL_l}{PL_l^{\max}} \right| \tag{6}$$

$$pn_2 = \sum_{l=1}^{NL} \left| \left| \frac{PL_l}{PL_l^{\max}} \right| - \frac{\sum_{l=1}^{NL} \left| PL_l / PL_l^{\max} \right|}{NL} \right| \tag{7}$$

The first penalty term denotes the absolute loading rate of weather affected lines. This term is introduced to adjust the power flow and avoid the weather affected lines undertaking heavy loads. The second penalty term denotes the mean absolute deviation (MAD) of lines load rate which is a measure of statistical dispersion defined as $\frac{1}{n}\sum_{k=1}^{n}|y_k - \bar{y}|$ where $\bar{y}$ is the mean of $\{y_1, y_2, \ldots, y_n\}$. pn_2 is established to reduce the power flow heterogeneity and the cascading risk when lines are subject to extreme events. By including the above two penalty terms, the transmission network is operating at a more resilient loading level. That is, each component on outage will have a lower impact on the physical system, which will have a larger operating margin in extreme conditions. Note that the term is nonconvex where its convexification and linearization methodology is proposed in the next subsection.

Our earlier work [26] presented a resilience-constrained unit commitment model where the power flow entropy was considered to improve the power system resilience. However, the two penalty terms proposed in [26] were approximated for improving the solution at the cost of lowering the optimality. In this paper, new penalty terms and solution methodology are proposed for enhancing the optimality. The penalty terms are simpler which will lead to faster computation performance.

B. Outage Set for RCED

In this paper, common-cause outages of two adjacent lines and cascading outages are considered to construct outage set. For common-cause outages, assuming that bus i has k connected lines and C_k^2 contingencies are added to this bus. Traverse all buses in the weather affected areas and establish the contingencies accordingly. Practically, there are few lines connected to one bus and the proposed common-cause outage contingencies will not lead to the curse of dimensionality. For cascading outages, the heavily loaded lines upon the weather-induced initial outage are identified and added into outage set in case of hidden outages.

Constraints corresponding to each outage are constructed using LODFs [23]. The corresponding contingency constraints for initial outages are shown in (8)-(9). Given that line $p$is on outage, the adjacent lines and those which are heavily loaded are denoted as q. The constraints for common-cause and cascading outages are shown in (10)-(11).

$$PL_l^{pc} = PL_l + LODF_{l,p}^{pc} \cdot PL_p \ \forall l, p \tag{8}$$

$$\left| PL_l^{pc} \right| \le PL_{\max,l} \tag{9}$$

$$PL_l^{p-q,c} = PL_l + LODF_{l,p}^{p-q,c} \cdot PL_p + LODF_{l,q}^{p-q,c} \cdot PL_q \quad \forall l, p, q \tag{10}$$

$$\left| PL_l^{p-q,c} \right| \le PL_{\max,l} \tag{11}$$

where PL_l^{pc} is line l flow due to line p outage. PL_l, PL_p and PL_q are steady-state flows on lines l, p and q, respectively. $PL_l^{p-q,c}$ is the line l flow due to common-cause outages of lines p and q. $LODF_{l,p}^{pc}$ is line outage distribution factor between flows on lines l and p when line p is on outage. $LODF_{l,p}^{p-q,c}$ and $LODF_{l,q}^{p-q,c}$ are line outage distribution factor between flows of lines l and lines p, and q, respectively.

The LODF of single and multiple outages are calculated by the following equations [31].

$$\mathbf{LODF_{M,O}} = \mathbf{PTDF_{M,O}^{0}}\left(\mathbf{E} - \mathbf{PTDF_{O,O}^{0}}\right)^{\mathbf{-1}} \tag{12}$$

$$\mathbf{PTDF_{M,O}^{0}} = \mathbf{X_M^{-1}\Phi^T[B]^{0-1}\Psi} \tag{13}$$

$$\mathbf{PTDF_{O,O}^{0}} = \mathbf{X_O^{-1}\Psi^T[B]^{0-1}\Psi} \tag{14}$$

where $\mathbf{E}$ is an identity matrix of $\nu \times \nu$, ν is the number of lines on outage. *PTDF* is power transfer distribution factor which determines the change in line flows when one unit of power is transferred from on bus to the next. $\mathbf{X_M}$ and $\mathbf{X_O}$ are diagonal matrices with elements representing the reactance of lines that are monitored and those on outage, respectively. $\mathbf{\Phi}$ is a bus-to-monitored line incidence matrix and $\boldsymbol{\psi}$ is bus-to-outaged line incidence matrix.

The contingency screening and the constraint construction process are shown in Fig. 4 and described as follows. The method starts by calculating the proposed RCED without contingency constraints and obtaining the pre-contingency line flows. Then the outage filter uses (8) and (10) based on LODF to calculate PL_l^{pc} and $PL_l^{p-q,c}$ for all post-contingency line l flows. The evaluation process will end if all post-contingency power flows are within limits. Otherwise, every combination of line p on outage and overloaded line l are

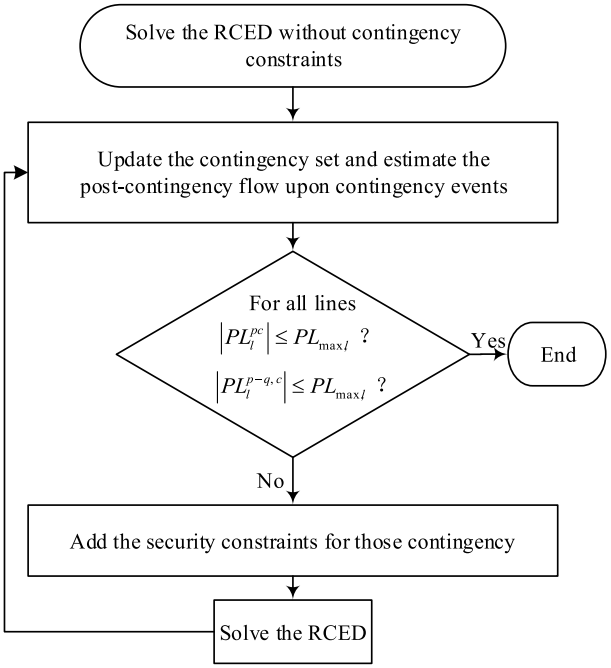

Fig. 4. Flowchart of LODF post-contingency filter for RCED.

stored and added to the RCED model using the corresponding constraints (8)-(9) or (10)-(11). The RCED solution will provide new pre-contingency flows which are analyzed to verify if additional combinations should be added to RCED. This iterative approach checks all lie outages in extreme events and common-cause outages of adjacent lines at each iteration. Then if the calculated line l flow, due to a line p outage or common-cause outages of lines p and q, is higher than the line l capacity, the corresponding outages will be added to RCED in the next iteration. In practice, it is expected that a limited list of active line outages will be required to establish a secure operation.

C. Proposed RCED Model

The proposed resilience-constrained economic dispatch model is formulated as follow with established penalty terms and contingency constraints.

$$\text{Min. } \alpha \cdot \sum_{i=1}^{NG} C_i(P_i) + \beta \cdot \sum_{l=S_{AL}} \left| \frac{PL_l}{PL_l^{\max}} \right| + \gamma \cdot \sum_{l=1}^{NL} \left| \left| \frac{PL_l}{PL_l^{\max}} \right| - \frac{\sum_{l=1}^{NL} \left| PL_l / PL_l^{\max} \right|}{NL} \right| + \eta \cdot \sum_{j}^{ND} LC_j \tag{15a}$$

$$\text{s.t. } C_i(\cdot) = a_i + b_i P_i + c_i P_i^2, \ \forall i \tag{15b}$$

$$\sum_{i}^{NG} P_i = \sum_{j}^{ND} \left(PD_j - LC_j \right) \tag{15c}$$

$$P_{\min,i} \le P_i \le P_{\max,i}, \forall i \tag{15d}$$

$$0 \le LC_j \le PD_j, \forall j \tag{15e}$$

$$\sum_{l}^{NL} KL_{b,l} \cdot PL_l = \sum_{i}^{NG} KP_{b,i} \cdot P_i - \sum_{j}^{ND} KD_{b,j} \cdot \left(PD_j - LC_j \right), \forall b \tag{15f}$$

$$PL_l = \frac{\theta_{fl} - \theta_{tl}}{x_l}, \forall l \tag{15g}$$

$$-PL_{\max,l} \le PL_l \le PL_{\max,l}, \forall l \tag{15h}$$

$$PL_l^{pc} = PL_l + LODF_{l,p}^{pc} \cdot PL_p, \forall l, p \tag{15i}$$

$$\left| PL_l^{pc} \right| \le PL_{\max,l}, \forall l \tag{15j}$$

$$PL_l^{p-q,c} = PL_l + LODF_{l,p}^{p-q,c} \cdot PL_p + LODF_{l,q}^{p-q,c} \cdot PL_q \forall l, p, q \tag{15k}$$

$$\left| PL_l^{p-q,c} \right| \le PL_{\max,l}, \forall l \tag{15l}$$

The model constraints are shown in (15b)-(15l) in which the common-cause and cascading outage constraints are included. Constraint (15c) ensures the power balance. Constraint (15d) limits the upper/lower bounds of generation output. Constraints (15e) limits the upper/lower bounds of load curtailment. Constraints (15f)-(15h) represent line power flows and capacity limits. Constraints (15i) and (15j) are constructed for implementing the N-1 contingency in weather-induced areas. Upon weather-induced initial outages, constraints (15k)-(15l) are constructed for considering common-cause and cascading outages.The proposed generation dispatch strategy could be applied to both day-ahead planning and intra-day time frame when extreme events are expected. In practice, the RCED approach could be implemented quickly which depends on the availability of powerful computers, advanced communication systems and power market mechanisms.

IV. Solution Methodology of RCED Model

Note that the non-convexity of the objective function (15a) is due to the nested absolute function of the third term. If we substitute $r_l = |\frac{PL_l}{PL_{\max,l}}|$ into (15a), the problem (15) yields to

$$\text{Min. } \alpha \cdot \sum_{i=1}^{NG} C_i(P_i) + \beta \cdot \sum_{l \in S_{AL}} r_l + \gamma \cdot \sum_{l=1}^{NL} \left| r_l - \frac{\sum_{l=1}^{NL} r_l}{NL} \right| + \eta \cdot \sum_{j}^{ND} LC_j \tag{15m}$$

$$s.t. \ (15b) - (15l) \tag{15n}$$

$$r_l = \left| \frac{PL_l}{PL_{\max,l}} \right|, \forall l \tag{15o}$$

A general optimization method is proposed in [26] to linearize the objective function with absolute value functions. Accordingly (16) yields to (17) while the optimal solution remains the same.

$$\text{Min. } \alpha \cdot \sum_{i=1}^{NG} C_i(P_i) + \beta \cdot \sum_{l \in S_{AL}} r_l + \gamma \cdot \sum_{l=1}^{NL} (u_l + v_l) + \eta \cdot \sum_{j}^{ND} LC_j \tag{16a}$$

$$s.t. \ (15b) - (15l) \tag{16b}$$

$$r_l - \frac{\sum_{l=1}^{NL} r_l}{NL} + u_l - v_l = 0, \forall l \tag{16c}$$

$$u_l \geq 0, v_l \geq 0, \forall l \tag{16d}$$

$$r_l = \left| \frac{PL_l}{PL_{\max,l}} \right|, \forall l \tag{16e}$$

In this paper, we further linearize constraints (16e) which include absolute functions without the loss of optimality.

Consider a more general form of the proposed mathematical programming model as

$$\text{min.} \quad F(\boldsymbol{x}) \tag{17a}$$

$$s.t. \quad g(\boldsymbol{x}) + \sum_{k=1}^{m} \left| \sum_{i=1}^{n} d_{k,i} x_i \right| = b \tag{17b}$$

$$\& \text{ other model constraints} \tag{17c}$$

Define auxiliary variables $s_k, t_k,\ k = 1, 2, \ldots, K$ to construct the model in (19).

$$\text{min.} \quad F(\boldsymbol{x}) \tag{18a}$$

$$\text{s.t.} \quad g(\boldsymbol{x}) + \sum_{k=1}^{k} (s_k + t_k) = b \tag{18b}$$

$$\sum_{i=1}^{n} d_{k,i} x_i = s_k - t_k, \quad k = 1, 2, \ldots, K \tag{18c}$$

$$s_k \geq 0, t_k \geq 0,\ k = 1, 2, \ldots, K \tag{18d}$$

$$\& \text{ other model constraints} \tag{18e}$$

Theorem 1: If $(\boldsymbol{x}, \boldsymbol{s}, \boldsymbol{t})$ is the feasible solution of the model in (18), the sufficient and necessary condition for x as the feasible solution of the model in (17) is $s_k t_k = 0, \forall k$.

Proof of necessity: If $(\boldsymbol{x}, \boldsymbol{s}, \boldsymbol{t})$ is the feasible solution of the model in (18) and x is the feasible solution of (17), then

$$\sum_{k=1}^{K} (s_k + t_k) = b - g(x) = \sum_{k=1}^{K} \left| \sum_{i=1}^{n} d_{k,i} x_i \right| = \sum_{k=1}^{K} |s_k - t_k| \tag{19}$$

The three equal signs in (19) are due to (18b), (17b) and (18c), respectively. Since $s_k \geq 0,\ t_k \geq 0$ we have

$$|s_k - t_k| \leq |s_k| + |t_k| = s_k + t_k \tag{20}$$

According to (19), (20), we have $|s_k - t_k| = s_k + t_k, \forall k$ Thus, at least one term in a pair of $S_k\ t_k$, is 0, i.e., $S_k\ t_k = 0$.

Proof of Sufficiency: If $(\boldsymbol{x}, \boldsymbol{s}, \boldsymbol{t})$ is the feasible solution of (18) and $S_k t_k = 0, \forall k$ then

$$s_k + t_k = |s_k - t_k| = \left| \sum_{i=1}^{n} d_{k,i} x_i \right| \tag{21}$$

The second equal sign is due to (18c). Substitute (21) into (18b), then (18b) yields to (17b). Therefore, x is the feasible solution of (18) when $s_k t_k = 0$, and $(\boldsymbol{x}, \boldsymbol{s}, \boldsymbol{t})$ is the feasible solution of (19). ■

Add the sufficient and necessary condition to (18) to get (22). The big-M method is used to relax $s_k t_k = 0, \forall k$.

$$\text{min.} \quad F(\boldsymbol{x}) \tag{22a}$$

$$s.t. \quad (18b) - (18e) \tag{22b}$$

$$0 \leq s_k \leq M \times \delta \tag{22c}$$

$$0 \leq t_k \leq M \times (1 - \delta) \tag{22d}$$

$$\delta \in \{0, 1\} \tag{22e}$$

Theorem 2: The optimal objective function value of (22) is equal to that of (17).

Proof: If x is the feasible solution of (17), it is also feasible in (18) since we can always assign s_k, t_k to make (18b) yield to (17b). Recalling theorem 1, we conclude that the feasible region of x in (22) is the same as that of (17). So, the optimal objective function value of (22) is exactly equal to that of (17), although the two models are not essentially equivalent. ■

According to theorem 2, problem (23) can be constructed with the same optimal solution as that of (17) which is equivalent to (16) and (15).

$$\text{Min.} \quad \alpha \cdot \sum_{i=1}^{NG} C_i(P_i) + \beta \cdot \sum_{l \in S_{AL}} r_l + \gamma \cdot \sum_{l=1}^{NL} (u_l + v_l) + \eta \cdot \sum_{j}^{ND} LC_j \tag{23a}$$

$$s.t. \quad \text{Original constraints: } (15b) - (15l) \tag{23b}$$

$$\text{Linearize (15m): } (16c) - (16d) \tag{23c}$$

$$\text{Linearize (15o): } \begin{cases} r_l = s_l + t_l \\ \frac{PL_l}{PL_{\max,l}} = s_l - t_l \end{cases}, \forall l \tag{23d}$$

$$\text{Ensure optimality: } \begin{cases} 0 \leq s_l \leq M \cdot \sigma_l \\ 0 \leq t_l \leq M \cdot (1 - \sigma_l) \\ \sigma_l \in \{0, 1\}. \end{cases}, \forall l \tag{23e}$$

V. Case Studies

A. Case Studies for the IEEE-30 Bus Test System

To verify the effectiveness of proposed model, the modified IEEE 30-bus system is introduced and tested in MATLAB 2016a using the Gurobi solver on a personal computer with a 3.20 GHz i5 processor and 8 GB RAM. The IEEE 30-bus system is composed of six generators, twenty-one loads and forty-one transmission lines. The test system parameters are available in http://motor.ece.iit.edu/data/RCED.xlsx.

Without loss of generality, all transmission lines are assumed to be exposed to the same weather conditions. We generate 1,000 scenarios in order to calculate blackout performance distributions.

The following four cases are discussed.

Case 1: Solve the model in (12) without considering any outages and load curtailment. This case is to study the regulating effects of penalty terms on the uniformity of power flow distribution.

Case 2: Based on the dispatch solution in Case 1, perform a resilience evaluation to calculate the proposed RI. This case is to verify the effectiveness of penalty terms and the rationality of the proposed RI.

Case 3: The introduced contingencies constraints are added to Case 2. System resilience is further studied using the proposed RCED model.

Case 4: Evaluate the impact of weather severities on system resilience.

For the sake of brevity, in the following discussion, NCED denotes the networked-constrained economic dispatch without penalty terms or contingencies constraints. SCED denotes the NCED with N-1 contingency constraints. RCED denotes the dispatch model with penalty terms. C-RCED denotes the dispatch model with both penalty terms and the contingencies constraints. We vary the objective function coefficients to consider the following two RCED models: RCED I with $\alpha = 1, \beta = 100, \gamma = 1000$; RCED II with $\alpha = 1, \beta = 1000, \gamma = 10000$. In case C-RCED I, $\eta = 200$. In case C-RCED II $\eta = 10000$. The results for the four cases are presented as follows.

Case 1: Case 1 is performed to verify the feasibility of linearization method and the effectiveness of the proposed penalty terms embedded in the RCED model. The optimization preference between generation cost and power flow distribution can be adjusted by varying β, γ. The two penalty terms are studied separately and the results are shown in Tables I. Table II shows the results with both penalty terms in place. Since the penalty terms are introduced to adjust the power flow, four indices are calculated including the average line loading rate (Ave.r_l), maximum line loading rate (Max.r_l), number of heavily loaded lines (Num.$r_l > 0.7$ for $r_l > 0.7$) and mean absolute deviation of line loading rate (MADr_l).

In Table I, four power flow distribution indices are improved when β is larger than 100. This is because when $\beta = 1$, pn_1 is 16.669 and the corresponding generation cost is \$8,495.18. As β increases, pn_1 becomes larger and makes up a higher proportion of the objective function. Thus, larger β which increases the generation cost, results in a more effective penalty term and more homogeneous power flow. When β is 10,000, the average loading rates are lowered to 0.304. However, the adjustment in power flow distribution is limited by generation and line capacities, network topology, system loading, etc. The results corresponding to $\beta = 100000$ are the same as those of $\beta = 10000$. In addition, MAD of r_l which represents the homogeneity of power flow distribution decreases first as β increases and then increases when β becomes very large. This outcome indicates that although the first penalty term can reduce the average loading rate, its impact on power flow distribution is not uniform.

The results for varying γ are also shown in Table I. Both MAD of r_l decrease as γ is increased. Compared with the results as β is varied, the smallest MAD is reduced by about 46%. Both the maximum loading rate and the number of heavily loaded lines are lower than that when β is varied. When $\gamma = 10000$, line loading rates are all below 0.7 with a maximum loading rate of 0.64. This is because heavily loaded lines will have a higher priority to be optimized in our case which would lower pn_2. However, the average loading rateis deteriorated which indicates that the two penalty terms fulfill different tasks for adjusting power flows.

Table II shows the comparison of conventional NCED and the proposed RCED in which the proposed RCED model performs better than the traditional NCED. In Table II, there are 5 lines with a loading rate that exceeds 0.7 while there is only one in RCED I and none in RCED II. Besides, the maximum r_l of NCED is 1, which indicates that certain lines are operated at their capacity which are more prone to hidden outages when power flows fluctuate, especially when line outages occur in extreme weather conditions. Even at higher dispatch costs, the operation security remains to be the primary consideration in extreme conditions.

TABLE I
RESULTS WHEN β, γ VARIES

	β varies, $\alpha = 1, \gamma = 0$				γ varies, $a = 1, \beta = 0$			
	Ave. r_l	MAD r_l	Max. r_l	Num. of $r_l > 0.7$	Ave. r_l	MAD r_l	Max. r_l	Num. of. $r_l > 0.7$
1	0.407	0.220	1.00	5	0.406	0.218	1.00	5
100	0.388	0.190	1.00	4	0.407	0.137	1.00	1
1000	0.315	0.173	0.87	3	0.367	0.097	0.75	1
10000	0.304	0.179	0.87	3	0.357	0.096	0.64	0
100000	0.304	0.179	0.87	3	0.357	0.096	0.64	0

TABLE II
RESULTS WHEN BOTH β AND γ VARY

Model	NCED	RCED I	RCED II
Gen. Cost (\$)	8495.17	8982.11 (+5.73%)	9219.44 (+8.52%)
Ave. r_l	0.407	0.366 (-10.07%)	0.356 (-12.50%)
Max. r_l	1.00	0.74	0.64
Num. of $r_l > 0.7$	5	1	0

Case 2: In this case, the three models, NCED, RCED I and RCED II, are tested without contingencies. Accordingly, reliability and resilience performances are compared and discussed. The weather condition is assumed to be a major storm at an average speed of 35 m/s. The wind-dependent line and tower outage probabilities are calculated according to fragility curves. The hidden outage probability is $p_0 = 0.02$ when $r_l \leq 1$ which increases to 1 when $r_l = 1.4$. The generation ramping limit is set at 10% on each island. The number of cascading scenarios in the resilience evaluation process is $k_{\max} = 1000$. The blackout size is denoted by (load curtailment/system load) $\times$ 100%.

Fig. 5 (a) shows the probability distribution of blackout size. Both RCED I and RCED II perform better than the traditional NCED. The maximum load curtailment percentage of NCED is 60%, while it is only 40% in RCED I and 30% in RCED II. Moreover, the probability distribution of NCED in Fig. 5 (a) shows a relatively flat tail when load curtailment percentage is over 30. To further investigate this situation, the log-log plot of blackout size is shown in the Fig. 5 (b). The NCED curve in Fig. 5 (b) shows the characteristics of power-law distribution with the power tails. A long flat tail generally implies a higher risk of large blackouts [28]. The two RCED curves drop exponentially with the blackout size in Fig. 5 (b). Therefore, the RCED model reduces the risk of large blackouts effectively by improving the power flow distribution.

Table III shows the outage results for NCED and RCED. The weather-induced outage scenarios are similar since the weather conditions are assumed identical for triggering

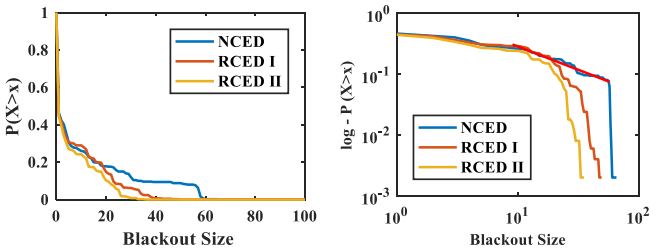

(a) In linear plot (b)In log-log plot

Fig. 5. Distribution of blackout size in NCED and RCED.

TABLE III
RESULTS IN DIFFERENT DISPATCH MODELS

Model	NCED	RCED I	RCED II
Generation Cost ($)	8,495.17	8,982.11	9,219.44
Weather-induced Outage Scenarios N_0	554	582	572
Hidden Outage Scenarios, N_h	186	78	74
Average Hidden Outage Lines	3.02	1.15	0.90
Expected Load Curtailment (%)	9.65	6.91	5.35
Resilience Index RI (%)	194.19	81.96	50.29

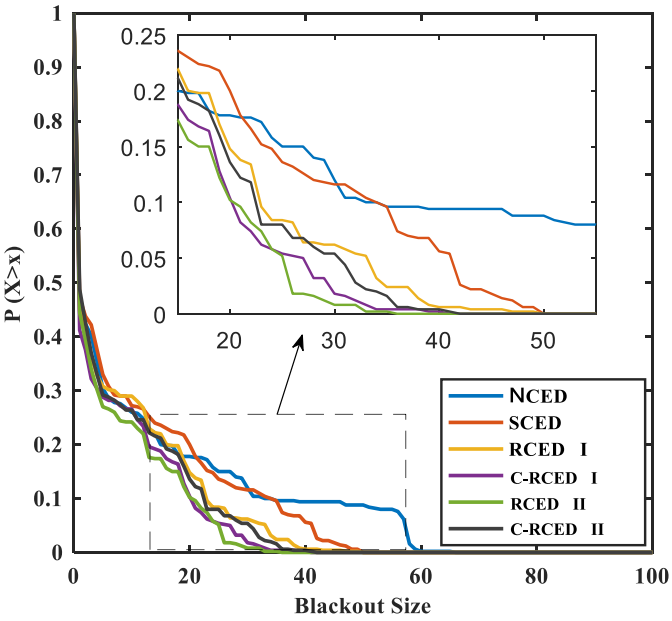

Fig. 6. Blackout size distribution in different models.

initial outages in the three models. However, different dispatch strategies could lead to various hidden outage scenarios and blackout sizes. There are 186 hidden outage scenarios in NCED while there are only 78 and 74 in RCED I and RCED II. Furthermore, the average numbers of lines with hidden outages are 3.02, 1.15 and 0.90, respectively. This indicates that both numbers of overload and hidden outage scenarios and lines are improved in the RCED models, even though the initial triggers are the same. Moreover, the proposed RI distinguishes the three models more effectively than expected load curtailment does. The expected load curtailment of RCED I and II are similar. However, their resilience indices are very different.

The traditional NCED aims to determine the least production operation cost of power systems but pays little attention to the power flow distribution. In this way, there could be a few dangerous states in which some of the transmission lines are heavy loaded in which any minor power flow fluctuations or transfers would lead to cascading outages. That situation will be magnified further under extreme events. The proposed RCED model can be adopted as a more resilient operation strategy under normal and extreme conditions for blackout prevention.

Case 3: In Case 3, the N-1, common-cause and cascading outage constraints are further added to illustrate its effect on blackout prevention. Based on the generation dispatch plan in Case 2, we follow the contingency check with an optimal load shedding model. It is not surprising that neither RCED I nor RCED II model used in Case 2 satisfies the outage constraints. The load curtailed in the two models are 24.9MW and 20.97MW, respectively, which indicate that an improved uniformity in power flow distribution cannot always ensure a higher reliability in response to typical outages. Hence, typical outages and penalty terms for power flow adjustment should be considered simultaneously in power dispatch strategies. In this case, buses 21-25 are located in extreme weather affected areas. We consider common-cause and cascading outages according to the description in Section III. Note that outages which would split the system are not active.

Fig. 6 shows the blackout size distribution in different models. Comparing NCED (in blue) and SCED with N-1 contingency (in red), the power tail of blue curve gets improved in the red case. However, the resilience in both NCED and SCED cases is still worse than that in RCED models due to higher proportion of large blackouts. Comparing RCED I (in yellow) with C-RCED I (in purple), we can see that the purple curve is lower than yellow, which means the common-cause outage constraints lead to less blackout and could improve the system resilience. On the contrary, the resilience of C-RCED II (in black) is worse than that of RCED II (in green).

In this case, contingency constraints pose negative effect on resilience. This observation indicates that the impact of contingency constraints on resilience is uncertain. The results show that the addition of contingency constraints might not always improve resilience and sometimes it could even make worse under certain circumstances. This interesting phenomenon can be explained in terms of the power flow distribution as shown in Table IV. Comparing the line flow distribution of different models, we encounter that the power flow distribution of RCED I is improved when contingency constraints are added. However, the distribution indices of RCED II are deteriorated when contingency constraints are added. Accordingly, contingency constraints can improve the power system resilience if they improve the power flow uniformity. This observation further demonstrates that the power system resilience has a close relationship with power flow distribution and the traditional SCED cannot prevent blackouts effectively with only the N-k reliability strategy is pursued.

TABLE IV
POWER FLOW DISTRIBUTION AND RI IN DIFFERENT MODELS

Model	Ave. r_l	Max. r_l	Num. of $r_l > 0.7$	ELC (MW)	*RI* (%)
RCED I	0.366	0.74	1	19.604	81.96
C-RCED I	0.354	0.73	1	15.938	56.96
RCED II	0.356	0.64	0	15.168	50.29
C-RCED II	0.354	0.793	1	18.331	70.79

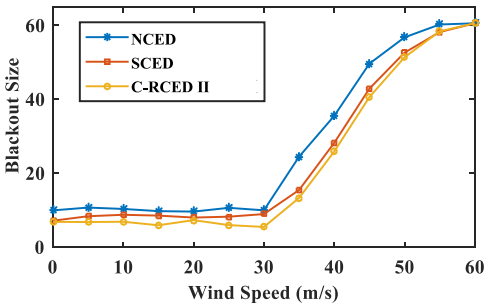

Fig. 7. Effect of wind speed on blackout size.

TABLE V
COMPUTATION TIME OF DIFFERENT DISPATCH STRATEGY AND RESILIENCE EVALUATION

Time(s)	RTS-96	IEEE 118	Polish 2383wp
NCED	0.25	0.39	4.06
RCED	100.34	150.16	322.07
C-RCED	496.45	500.93	856.35
RI calculation	134.17	153.99	14469.02

Case 4: Case 4 studies the influence of wind speed on resilience. This case helps find the effectiveness of dispatch strategies when weather condition varies. Fig. 7 shows the expected LC percentage over all scenarios for different wind speeds in which the system is resilient (i.e., LC percentage is under 10%) when wind speed is below 30m/s. The LC percentage has a sharp increase as wind speed increases. For wind speed below 40m/s, the LC percentage in the proposed C-RCED is obviously below that of NCED and SCED. As wind speed increases, the gap between C-RCED and SCED becomes smaller which indicates that the operational strategy would have a weaker influence on the system resilience. When the wind speed is over 60m/s, there is no difference among dispatch strategies. That is, the resilience cannot be improved by enhancing the operational strategies. However, the infrastructural improvements, such as hardening of lines and towers will have a more profound impact on resilience when extreme events become destructive.

B. Case Studies on Large Test Systems

The added penalty terms and contingency constraints are suitable for large power systems. To show the computational efficiency and validity, we apply the model to more complicated test systems, including the RTS-96, the IEEE 118 bus and the Polish 2383wp test case. The network parameters and load data of the RTS-96 test system are provided in [32], and the parameters of the IEEE 118 bus and the Polish 2383wp test systems are provided by Matpower 5.0.

TABLE VI
LOAD FLOW DISTRIBUTION AND RESILIENCE INDEX FOR DIFFERENT STRATEGIES IN RTS-96 TEST SYSTEM

Model	NCED	RCED	C-RCED
Generation Cost ($)	102576	195102	195617
Ave. r_l	0.4956	0.2330	0.2329
Max. r_l	1	0.639	0.667
Number of $r_l > 0.7$	32	0	0
Max. LC	61.64%	37.08%	30.39%
Resilience Index	317.04	102.84	45.16

TABLE VII
LOAD FLOW DISTRIBUTION AND RESILIENCE INDEX FOR DIFFERENT STRATEGIES IN POLISH 2383WP TEST SYSTEM

Model	NCED	RCED	C-RCED
Generation Cost ($)	1799364	1885083	1883980
Ave. r_l	0.3524	0.3381	0.321
Max. r_l	1	1	1
Number of $r_l > 0.7$	360	307	286
Max. LC	22.94%	17.68%	13.87%
Resilience Index	42.42	17.26	9.85

The three test system parameters used in this paper are available at http://motor.ece.iit.edu/data/RCED.xlsx. In the RCED case, for the RTS-96 test system $\alpha = 1$, $\beta = 10000$, $\gamma = 10000$, and for the IEEE 118-bus test system and the Polish 23832wp test systme $\alpha = 1$, $\beta = 100000$, $\gamma = 100000$. In the C-RCED case, for all test systems, $\eta = 5000$, and the buses affected by extreme weather are No. 113, 117, 120, 124, 203, 204, 205, 206, 207, 208, 209, 210, and 211 for the RTS-96 test systems, No. 98, 99, 100, 103, 104, 105 and 107 for the IEEE 118-bus test system, and No. 100 to 125 for the Polish 2383wp test system.

We consider N-1 and common-cause outages according to the description given in Section III for each case and estimate post-contingency flows. Those lines whose post-contingency flow rates exceed 0.85 are selected to initiate cascading outages. Note that contingencies which would split the system are not considered in resilience evaluations. The wind power flow through affected lines would have a random speed ranging from 30m/s to 45m/s in all cases. Table V demonstrates the computation time of the proposed method for different test systems and the simulation time for the RI evaluation. In Table V, the proposed penalty terms and common-cause outage constraints will result in a longer computing time. However, the computation time even for the Polish 2383wp test system is still within the acceptable range of the scheduling department.

Tables VI and VII demonstrate the load flow distribution and RI using the proposed strategy and the conventional NCED for the TRS-96 and the Polish 2383wp test system, respectively. Figs. 8(a) and 8(b) show the blackout size distribution

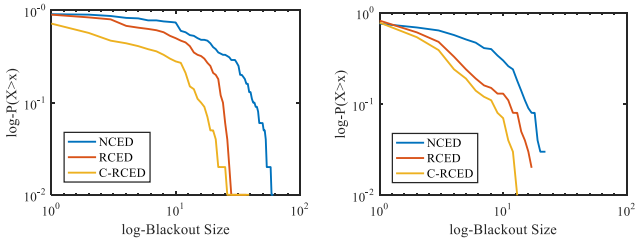

(a) RTS-96 (b) Polish 2383wp

Fig. 8. Blackout size distribution for different strategies in TRS-96 and Polish 2383wp test system.

for different strategies applied to RTS-96 and Polish 2383wp test systems, respectively. In Tables VI and VII, the load flow derived from the proposed RCED and C-RCED models are better than that of NCED. The maximum loading rate in NCED is up to 1 for both the RTS-96 and the Polish 2383wp test systems, while they are reduced to 0.675 and 0.741 for the RTS-96 test systems in RCED, respectively. The heavy loaded lines in RCED and C-RCED are fewer than that in NCED. In Fig. 8, the blackout size distributions in the proposed strategies are fewer than that in NCED. Also, C-RCED performs better than RCED considering preventive contingency constraints. The RI for NCED, RCED and C-RCED in the Polish 2383wp test system are 42.42, 17.26 and 9.85, respectively. The RI for C-RCED is much smaller than that in NCED, which indicates that there are fewer large blackouts in C-RCED when the power system is encountering extreme weather. In Table VII, the maximum blackout size in C-RCED is 13.87% over 1000 scenarios while it is 22.94% for NCED.

VI. Conclusion

This paper proposes a resilience-constrained economic dispatch and the corresponding set of resilience indices for enhancing the resilience and blackout prevention. The following conclusions can be drawn.

- The proposed resilience indices demonstrate the power system adaptability to extreme events and distinguish different dispatch strategies even if their load curtailments are similar. The proposed indices can serve as adaptation indices in resilience evaluation effectively.
- The N-k reliability strategy cannot always obtain a better resilience, especially when a power system is subject to extreme events. On the contrary, the N-k reliability strategy can make the system resilience performance worse in certain cases. The impact of N-k strategy on resilience may also depend on power flow distribution.
- The proposed RCED simultaneously considers outage set and power flow distribution uniformity. The synergy of penalty terms and contingency constraints can achieve higher system resilience in extreme conditions.
- During extreme weather conditions, the effectiveness of operation strategies becomes less critical than those of infrastructural enhancement for resilience.

References

[1] M. Papic, S. Agarwal, J. Bian, and R. Billinton, "Effects of dependent and common mode out-ages on the reliability of bulk electric system—Part I: Basic concepts," in *Proc. IEEE PES Gen. Meeting Conf. Expo.*, National Harbor, MD, USA, 2014, pp. 1–5.

[2] R. Billinton, T. K. P. Medicherla, and M. S. Sachdev, "Application of common-cause outage models in composite system reliability evaluation," *IEEE Trans. Power App. Syst.*, vol. PER-1, no. 7, p. 62, Jul. 1981.

[3] R. Billinton and R. N. Allan, *Reliability Evaluation of Power Systems*, 2nd ed. New York, NY, USA: Plenum, 1996.

[4] A. Khodaei, "Provisional microgrids," *IEEE Trans. Smart Grid*, vol. 6, no. 3, pp. 1107–1115, May 2015.

[5] A. Gholami, T. Shekari, F. Aminifar, and M. Shahidehpour, "Microgrid scheduling with uncertainty: The quest for resilience," *IEEE Trans. Smart Grid*, vol. 7, no. 6, pp. 2849–2858, Nov. 2016.

[6] Z. Li, M. Shahidehpour, F. Aminifar, A. Alabdulwahab, and Y. Al-Turki, "Networked microgrids for enhancing the power system resilience," *Proc. IEEE*, vol. 105, no. 7, pp. 1289–1310, Jul. 2017.

[7] B. A. Carreras, D. E. Newman, I. Dobson, and A. B. Poole, "Evidence for self-organized criticality in a time series of electric power system blackouts," *IEEE Trans. Circuits Syst. I, Reg. Papers*, vol. 51, no. 9, pp. 1733–1740, Sep. 2004.

[8] I. Dobson, B. A. Carreras, V. E. Lynch, and D. E. Newman, "Complex systems analysis of series of blackouts: Cascading failure, critical points, and self-organization," *Chaos Interdiscipl. J. Nonlin. Sci.*, vol. 17, no. 2, Jun. 2007, Art. no. 026103.

[9] Y. Koç, M. Warnier, R. E. Kooij, and F. M. Brazier, "An entropy-based metric to quantify the robustness of power grids against cascading failures," *Safety Sci.*, vol. 59, pp. 126–134, Nov. 2013.

[10] Z. J. Bao, Y. J. Cao, G. Z. Wang, and L. J. Ding, "Analysis of cascading failure in electric grid based on power flow entropy," *Phys. Lett. A*, vol. 273, no. 34, pp. 3032–3040, Aug. 2009.

[11] M. Panteli, P. Mancarella, D. N. Trakas, E. Kyriakides, and N. D. Hatziargyriou, "Metrics and quantification of operational and infrastructure resilience in power systems," *IEEE Trans. Power Syst.*, vol. 32, no. 6, pp. 4732–4742, Nov. 2017.

[12] C. Nan and G. Sansavini, "A quantitative method for assessing resilience of interdependent infrastructures," *Rel. Eng. Syst. Safety*, vol. 157, pp. 35–53, Jan. 2017.

[13] M. Ouyang and L. Dueñas-Osorio, "Multi-dimensional hurricane resilience assessment of electric power systems," *Struct. Safety*, vol. 48, pp. 15–24, May 2014.

[14] C. Wang, Y. Hou, F. Qiu, S. Lei, and K. Liu, "Resilience enhancement with sequentially proactive operation strategies," *IEEE Trans. Power Syst.*, vol. 32, no. 4, pp. 2847–2857, Jul. 2017.

[15] Y. Jia, Z. Xu, L. L. Lai, and K. P. Wong, "Risk-based power system security analysis considering cascading outages," *IEEE Trans. Ind. Informat.*, vol. 12, no. 2, pp. 872–882, Apr. 2016.

[16] C. M. Rocco, J. E. Ramirez-Marquez, D. E. Salazar, and C. Yajure, "Assessing the vulnerability of a power system through a multiple objective contingency screening approach," *IEEE Trans. Rel.*, vol. 60, no. 2, pp. 394–403, Jun. 2011.

[17] T. Ding, C. Li, C. Yan, F. Li, and Z. Bie, "A bi-level optimization model for risk assessment and contingency ranking in transmission system reliability evaluation," *IEEE Trans. Power Syst.*, vol. 32, no. 5, pp. 3803–3813, Sep. 2017.

[18] A. Gholami, T. Shekari, and S. Grijalva, "Proactive management of microgrids for resiliency enhancement: An adaptive robust approach," *IEEE Trans. Sustain. Energy*, vol. 10, no. 1, pp. 470–480, Jan. 2019.

[19] X. Liu, M. Shahidehpour, Z. Li, X. Liu, Y. Cao, and Z. Bie, "Microgrids for enhancing the power grid resilience in extreme conditions," *IEEE Trans. Smart Grid*, vol. 8, no. 2, pp. 589–597, Mar. 2017.

[20] S. Ma, B. Chen, and Z. Wang, "Resilience enhancement strategy for distribution systems under extreme weather events," *IEEE Trans. Smart Grid*, vol. 9, no. 2, pp. 1442–1451, Mar. 2018.

[21] X. Wang, Z. Li, M. Shahidehpour, and C. Jiang, "Robust line hardening strategies for improving the resilience of distribution systems with variable renewable resources," *IEEE Trans. Sustain. Energy*, vol. 10, no. 1, pp. 386–395, Jan. 2019.

[22] L. Che, X. Liu, and Z. Li, "Screening hidden N-*k* line contingencies in smart grids using a multi-stage model," *IEEE Trans. Smart Grid*, vol. 10, no. 2, pp. 1280–1289, Mar. 2019. doi: 10.1109/TSG.2017.2762342.

[23] D. A. Tejada-Arango, P. Sánchez-Martın, and A. Ramos, "Security constrained unit commitment using line outage distribution factors," *IEEE Trans. Power Syst.*, vol. 33, no. 1, pp. 329–337, Jan. 2018.

[24] C. Shao, M. Shahidehpour, X. Wang, X. Wang, and B. Wang, "Integrated planning of electricity and natural gas transportation systems for enhancing the power grid resilience," *IEEE Trans. Power Syst.*, vol. 32, no. 6, pp. 4418–4429, Nov. 2017.
[25] M. Panteli, D. N. Trakas, P. Mancarella, and N. D. Hatziargyriou, "Power systems resilience assessment: Hardening and smart operational enhancement strategies," *Proc. IEEE*, vol. 105, no. 7, pp. 1202–1213, Jul. 2017.
[26] Y. F. Wang, L. P. Huang, M. Shahidehpour, L. L. Lai, H. L. Yuan, and F. Y. Xu, "Resilience-constrained hourly unit commitment in electricity grids," *IEEE Trans. Power Syst.*, vol. 33, no. 5, pp. 5604–5614, Sep. 2018.
[27] W. Li and R. Billinton, "Common cause outage models in power system reliability evaluation," *IEEE Trans. Power Syst.*, vol. 18, no. 2, pp. 966–968, May 2003.
[28] J. Chen, J. S. Thorp, and I. Dobson, "Cascading dynamics and mitigation assessment in power system disturbances via a hidden failure model," *Int. J. Elect. Power Energy Syst.*, vol. 27, no. 4, pp. 318–326, 2005.
[29] J. S. Thorp, A. G. Phadke, S. H. Horowitz, and S. Tamronglak, "Anatomy of power system disturbances: Importance sampling," *Int. J. Elect. Power Energy Syst.*, vol. 20, no. 2, pp. 147–152, 1998.
[30] B. A. Carreras, D. E. Newman, and I. Dobson, "North American blackout time series statistics and implications for blackout risk," *IEEE Trans. Power Syst.*, vol. 31, no. 6, pp. 4406–4414, Nov. 2016.
[31] J. Guo, Y. Fu, Z. Li, and M. Shahidehpour, "Direct calculation of line outage distribution factors," *IEEE Trans. Power Syst.*, vol. 24, no. 3, pp. 1633–1634, Aug. 2009.
[32] C. Grigg *et al.*, "The IEEE reliability test system-1996," *IEEE Trans. Power Syst.*, vol. 14, no. 3, pp. 1019–1020, Aug. 1999.

Yifei Wang (M'14) received the B.Eng. degree in electrical engineering from the North China University of Water Resource and Electric Power, the M.Sc. degree in electrical engineering from Wuhan University, and the Ph.D. degree in electrical engineering from Zhejiang University. He is currently an Assistant Professor with the School of Electrical Engineering, Southeast University, Nanjing, China, and a Visiting Scholar with the Electrical and Computer Engineering Department, Illinois Institute of Technology. His research interests include convex optimization in power systems, power system operation, and economics. He serves as an Associate Editor for the *Journal of Mordern Power System* and *Clean Energy*.

Liping Huang (S'16) received the B.Eng. degree from the China University of Mining and Technology, Beijing, China, in 2016. She is currently pursuing the Ph.D. degree with the School of Automation, Guangdong University of Technology, Guangzhou, China. She is a visiting Ph.D. student with the Electrical and Computer Engineering Department, Illinois Institute of Technology. Her research interests are in power system optimal operation and control, reliability, and resilience evaluation.

Mohammad Shahidehpour (S'79–M'81–SM'86–F'01) is the Bodine Chair Professor and the Director of the Robert W. Galvin Center for Electricity Innovation, Illinois Institute of Technology, Chicago, IL, USA. He was a recipient of the IEEE PES Ramakumar Family Renewable Energy Excellence Award, the IEEE PES Douglas M. Staszesky Distribution Automation Award, and the IEEE PES Outstanding Educator Award. He is a fellow of the American Association for the Advancement of Science and the National Academy of Inventors, and a member of the U.S. National Academy of Engineering.

Loi Lei Lai (SM'92–F'07) received the B.Sc. and Ph.D. degrees from the University of Aston and the D.Sc. degree from the City, University of London. He is currently a University Distinguished Professor with the Guangdong University of Technology, Guangzhou, China. He was the Director of Research and Development Centre, the Pao Yue Kong Chair Professor, the Vice President, a Professor and the Chair of electrical engineering, and a Fellow Committee Evaluator for State Grid Energy Research Institute, China; Zhejiang University, China; IEEE Systems, Man and Cybernetics Society (IEEE/SMCS); City, University of London; and IEEE Industrial Electronics Society, respectively. He was a recipient of the IEEE Third Millennium Medal, the IEEE Power and Energy Society (IEEE/PES) UKRI Power Chapter Outstanding Engineer Award in 2000, the IEEE/PES Energy Development and Power Generation Committee Prize Paper in 2006 and 2009, the IEEE/SMCS Outstanding Contribution Award in 2013 and 2014, and the Most Active Technical Committee Award in 2016. He is a fellow of IET, a National Distinguished Expert in China, and the Distinguished Expert in State Grid Corporation of China.

Ya Zhou (M'19) received the Doctoral degree in energy and environmental engineering from North China Electric Power University. She is currently an Associate Professor with the Guangdong University of Technology. She is currently a Visiting Scholar with the University of East Anglia. Her research focuses on energy system analysis, power system optimization, and environmental economics and sustainability. She is a member of International Society for Environmental Information Science.